1-1-1996

Destabilizing effect of proline substitutions in two helical regions of T4 lysozyme: Leucine 66 to proline and leucine 91 to proline

Terry M. Gray
Calvin University

Eric J. Arnoys
Calvin University

Stephen Blankespoor
Calvin University

Tim Born
Calvin University

Protein Science (1996), 5:742–751. Cambridge University Press. Printed in the USA.

Destabilizing effect of proline substitutions in two helical regions of T4 lysozyme: Leucine 66 to proline and leucine 91 to proline

TERRY M. GRAY, ERIC J. ARNOYS,[1] STEPHEN BLANKESPOOR,[2] TIM BORN,[3] REBEKAH JAGAR,[4] REBECCA EVERMAN,[5] DARLA PLOWMAN,[6] ANGELA STAIR, AND DAISY ZHANG[7]

Department of Chemistry and Biochemistry, Calvin College, Grand Rapids, Michigan 49546

(RECEIVED June 29, 1995; ACCEPTED January 17, 1996)

Abstract

A class of temperature-sensitive (ts) mutants of T4 lysozyme with reduced activity at 30 °C and no activity at 43 °C has been selected. These mutants, designated "tight" ts mutants, differ from most other T4 lysozyme mutants that are active at 43 °C, but only manifest their ts lesion by a reduced halo size around phage plaques after exposure of the growth plates to chloroform vapors. For example, in the series of T4 lysozyme mutants at position 157, the original randomly selected mutant, T157I, is the least stable of the series, yet, apart from the halo assay and subsequent in vitro protein stability measurements, this mutant is indistinguishable from wild type (WT) even at 43 °C.

Two mutants were identified: L91P and L66P. Both insert proline residues into α-helical regions of the WT protein structure. The stabilities ($\Delta\Delta G$) as determined by urea denaturation are 8.2 kcal/mol for L91P and 7.1 kcal/mol for L66P. CD spectra indicate that no major conformational changes have occurred in the mutant structures. The structures of the mutants were modeled with a 40-ps molecular dynamics simulation using explicit solvent. For L91P, the reduction of stability appears to be due to an unsatisfied hydrogen bond in the α-helix and to a new buried cavity. For L66P, the reduction of stability appears to be due to a disruption of the interdomain α-helix, at least two unsatisfied hydrogen bonds, and a newly formed solvent-filled pocket that protrudes into the hydrophobic core, possibly reducing the stabilizing contribution of a partially buried intrachain salt bridge.

Keywords: proline substitution; temperature-sensitive mutants; T4 lysozyme; protein stability; CD; UV difference spectroscopy; molecular dynamics; cavity

T4 lysozyme has become a model system for studies on the relationship among protein structure, stability, and sequence. The first studied mutants of T4 lysozyme were those obtained by means of random chemical mutagenesis of bacteriophage T4 followed by a screening of a large number of mutants using the lysoplate assay of Streisinger et al. (1961). Recent studies have used site-directed mutagenesis to rationally design mutants of T4 lysozyme (Matthews, 1987a; Blaber et al., 1994; Heinz et al., 1994). We have selected a class of temperature-sensitive (ts) mutants of T4 lysozyme with reduced activity at 30 °C and no activity at 43 °C. These mutants, designated tight ts mutants, are of special interest because the extreme phenotype is likely the result of major structural changes in the protein. These mutants differ from most other T4 lysozyme mutants that are active at 43 °C, but only manifest their ts lesion by a reduced halo size around phage plaques after exposure of the growth plates to chloroform vapors. For example, in the series of T4 lysozyme mutants at position 157 generated by Alber et al. (1987), the original randomly selected mutant, T157I (Grütter et al., 1987), is the least stable of the series, yet, apart from the halo assay and subsequent in vitro protein stability measurements, this mutant is indistinguishable from wild type (WT) even at 43 °C.

We report here two of these mutants: leucine 66 replaced with proline (L66P) and leucine 91 replaced with proline (L91P).

Reprint requests to: Terry M. Gray, Department of Chemistry and Biochemistry, Calvin College, Grand Rapids, Michigan 49546; e-mail: grayt@calvin.edu.

[1] Present address: Department of Biochemistry, Michigan State University, Lansing, Michigan 48824.

[2] Present address: Graduate Group in Bioengineering, University of California at Berkeley, Berkeley, California 94720.

[3] Present address: Department of Biochemistry and Molecular Biology, Mayo Graduate School of Medicine, Rochester, Minnesota 55905.

[4] Present address: Department of Mathematics, University of Notre Dame, Notre Dame, Indiana 46556.

[5] Present address: Department of Geology, University of Wisconsin, Madison, Wisconsin 53706.

[6] Present address: Department of Chemistry and Biochemistry, University of Colorado, Boulder, Colorado 80309.

[7] Present address: Department of Chemistry, Northern Arizona University, Flagstaff, Arizona 86011.

Both of these mutants introduce a new proline into T4 lysozyme. Leucine 66 is in the middle of the long interdomain α-helix of residues 60–80. Leucine 91 is the C-terminal residue of the α-helix of residues 83–90 (91). In general, proline is important in the kinetics of protein folding and often is responsible for a slow step due to *cis–trans* isomerization. The role of proline in stabilizing or destabilizing protein structure is less clear. Proline is a helix breaker in terms of its hydrogen bonding capabilities and the bulkiness of its side chain near the backbone, and is expected to destabilize protein structure in an α-helix (Barlow & Thornton, 1988). However, in T4 lysozyme, replacing the helical proline 86 with other amino acid residues does not result in increasing the stability of the protein even though normal hydrogen bonding and helical geometry is restored (Alber et al., 1988). This has been attributed to the fact that proline, with its restricted conformation, stabilizes the protein by reducing the entropy of the unfolded state (Matthews et al., 1987; Nicholson et al., 1992). According to theoretical (Yun et al., 1991) and experimental studies (O'Neil & DeGrado, 1990; Sauer et al., 1992), the cost of introducing a proline into an α-helix is around 3.4 kcal/mol.

Results

Mutagenesis, selection, and identification of amino acid substitutions

Following mutagenesis by 2-aminopurine, enrichment for tight ts mutants, and re-screening of the selected mutants, there were 28 with the tight ts phenotype. These make small plaques and no halos at 33 °C and no plaques at 43 °C. At 43 °C, plaque-forming ability is restored by adding hen eggwhite lysozyme. Of these 28 mutants, 6 have been cloned and sequenced. Two different substitutions have been identified: T to C at position 272 in the nucleotide sequence and T to C at position 197 in the nucleotide sequence. (Data not shown; the sequence numbering is as in Owen et al. [1983].) These correspond to amino acid substitutions leucine 91 to proline and leucine 66 to proline, respectively. The L91P mutation has appeared twice in the collection, and the L66P mutation has appeared four times.

Enzyme activity

Plaque-forming ability and halo size is one measure of the enzyme activity. At 33 °C, the small plaque size and the absence of any halo formation indicates a severe reduction of enzyme activity. Using the turbidometric assay at 25 °C, both L66P and L91P showed only a slight reduction of enzyme activity compared to WT. The activity of L91P was 74.9% of WT; the activity of L66P was 54.8% of WT.

Thermal denaturation

T4 lysozyme loses activity irreversibly when incubated at high temperatures (e.g., 65 °C). Relative protein stability can be determined by the rate of loss of activity: 75% of the enzyme activity was lost in 12 min for WT, in 1 min for L91P, and in 0.5 min for L66P. The stability of the mutant proteins is reduced significantly compared to the WT.

Urea-induced denaturation

Denaturation curves for WT, L91P, and L66P T4 lysozymes are shown in Figure 1. An analysis of these denaturation curves gives the midpoint of the unfolding transition ($[\text{urea}]_{1/2}$), the $\Delta G_{\text{unfolding}}$, and the *m*-value. These values are listed in Table 1. Also given is the stability of the mutant protein relative to WT ($\Delta\Delta G$). Because the stability of most T4 lysozyme mutants has been assessed by thermal denaturation methods, it is also useful to give the estimated T_m. This has been calculated using the $\Delta\Delta G$'s obtained from the urea denaturation analysis and the relationship $\Delta\Delta G = \Delta T_{m\Delta S}$ (Becktel & Schellman, 1987), assuming a ΔS of 320 cal/deg mol. Technically, this relationship holds only for small $\Delta\Delta G$'s and ΔT_m's. The value for L91P is consistent with that reported by Klemm et al. (1991) using urea gradient gel electrophoresis.

CD spectra

The CD spectra of L66P and L91P are nearly identical to the CD spectrum of WT T4 lysozyme with minima at 208 nm and 222 nm, indicative of a structure with significant α-helical structure (Fig. 2). Compared to the WT spectrum, the spectrum for L91P (Fig. 2C) has a slight qualitative difference, with deeper minimum at 208 nm, indicating slightly less α-helical structure and more random coil. This could be due either to a local disordering of the folded structure or to the presence of irreversibly unfolded chains in the sample.

Computer modeling

To determine the degree of equilibration of the molecular dynamics simulation, the calculated total energy and potential energy of the system was plotted as a function of time. Figure 3 shows such a plot for the L91P simulation; the other three simulations look very similar. After the initial warming to the target temperature, the simulation is quite stable during the entire time course. There seems to be a slight decrease in both energy

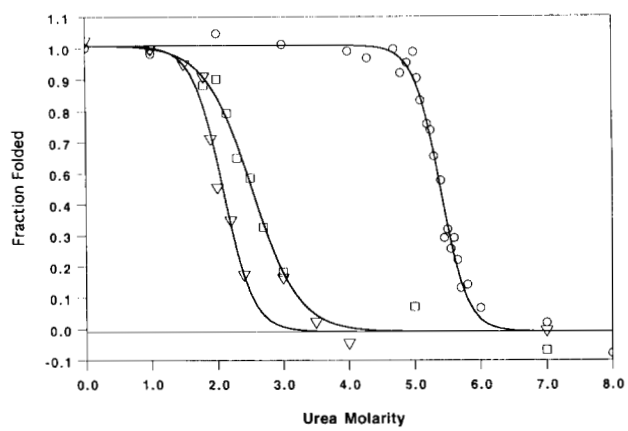

Fig. 1. Urea denaturation curves for WT (○), L66P (□), and L91P (▽) T4 lysozyme as determined by UV difference spectroscopy. The raw UV difference signal was converted to fraction unfolded using the baseline slopes and intercepts as determined by the nonlinear least-squares analysis.

Table 1. *Parameters characterizing the urea unfolding of T4 lysozyme and two mutants at 25 °C, pH 7.0, in 10 mM potassium phosphate buffer*

Protein	$\Delta G(H_2O)$[a] (kcal/mol)	m[a] (kcal/mol/M)	$[urea]_{1/2}$[a] (M)	$\Delta\Delta G$ (kcal/mol)	ΔT_m[b] (°C)
WT	16.55 (13.40)[c]	3.065	5.40		
L91P	5.57 (5.19)	2.670	2.09	10.98 (8.21)[c]	−34.3 (−25.7)[c]
L66P	4.32 (6.28)	1.708	2.53	12.23 (7.12)	−38.2 (−22.3)

[a] A least-squares analysis was used to determine the parameters in Equation 1: $[urea]_{1/2} = \Delta G(H_2O)/m$ = the midpoint of the denaturation curve.
[b] $\Delta T_m = \Delta\Delta G/\Delta S_m$ (WT) (Becktel & Schellman, 1987). For WT, $T_m = 65$ °C and $\Delta S_m = 320$ cal/mol deg.
[c] Values in parentheses are calculated using the average m value for all three proteins, 2.481 kcal/mol/M.

terms during the first 10 ps, after which there is very little change. The simulation is essentially equilibrated by the 10-ps time point. Consequently, the structures averaged over the 10–20-ps timeframe and the 20–40-ps timeframe represent equilibrium structures.

The D72P simulation resulted in a structure that was very similar to the 1L76 crystal structure in the vicinity of the proline mutation. In the WT structure, Asp 72 is a surface residue. Changing it to proline has very little effect except in the local backbone structure. In the mutant crystal structure, a slight kink is introduced into the α-helix at the site of the substitution. This is modeled accurately by molecular dynamics simulation.

Table 2 gives the RMS deviations (RMSDs) when the WT crystal structure (Weaver & Matthews, 1987) is compared to the WT structure derived from the dynamics simulation and to the two mutant structures also derived from the dynamics simulation. The crystal structure for the mutant D72P (Sauer et al., 1992) and the structure of D72P derived from the dynamics simulation are also included in the comparisons as an additional control to assess the reliablility of the structures determined by the dynamics simulation. There are two structures for each simulation: one generated by averaging structures between 10 and 20 ps of the simulation, and one generated by averaging structures between 20 and 40 ps of the simulation. Only backbone atoms were used in the RMS calculation. Not surprisingly, the RMSDs are larger for the 20–40-ps average structure (Table 2, upper right half of each section). The RMSD for the comparisons between the two crystal structures (3LZM versus 1L76) is very small relative to the comparisons between simulated structures. Although these small numbers are typical for RMSDs for comparisons of T4 lysozyme variants, these numbers may be artificially small because the WT coordinates (omitting the mutated residue) are typically used to generate the starting phases for the structure determination of the mutant T4 lysozymes. Table 2 also gives the RMS calculation when only one domain or the other is used in the comparison and shows a decrease in the RMSDs by 0.1–0.2 Å. This is consistent with a hinge motion that has been observed both experimentally (Faber & Matthews, 1990; Dixon et al., 1992) and computationally (Arnold et al., 1994). Figures 4 and 5 show the calculated WT structure superimposed onto the respective calculated mutant structure in the immediate neighborhood of the mutation using the 10–20-ps average structure in each case. The 10–20-ps average structures differ very little from the 20–40-ps average structures in the vicinity of the mutations (data not shown).

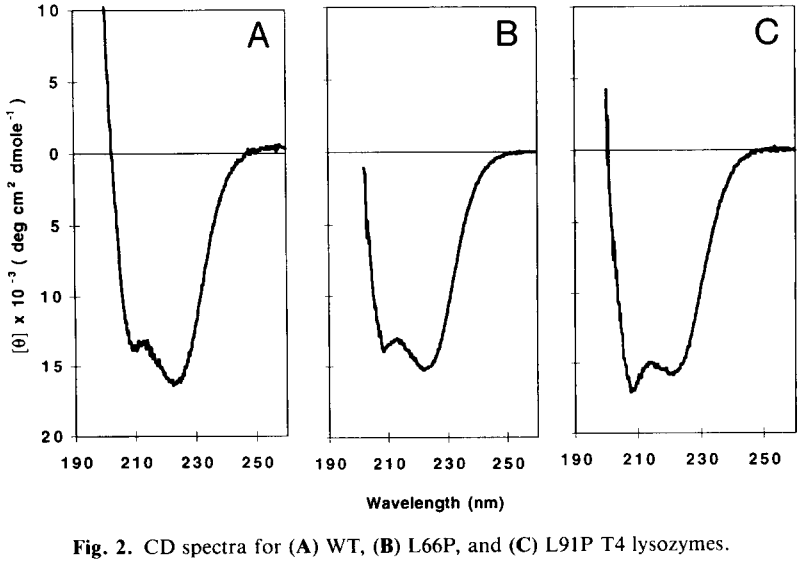

Fig. 2. CD spectra for (**A**) WT, (**B**) L66P, and (**C**) L91P T4 lysozymes.

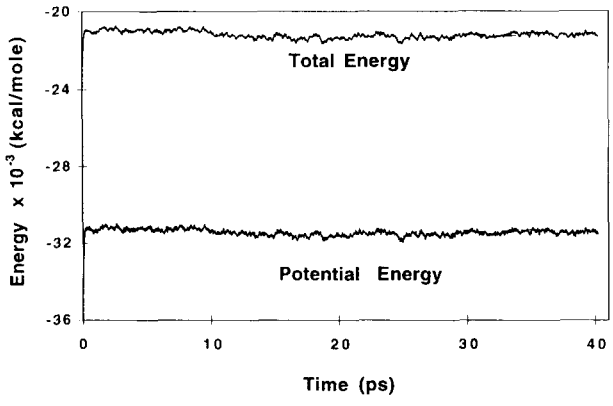

Fig. 3. Calculated potential energy and kinetic energy as a function of time for all solvent molecules and the L91P protein in the molecular dynamics simulation.

Discussion

The selection for "tight" ts mutants of T4 lysozyme has resulted in two mutants that are exceptionally destabilized compared to the WT protein: L91P and L66P. The $\Delta\Delta G$ values (8.2 and 7.1 kcal/mol, respectively) are among the largest known for any single amino acid substitution. The corresponding estimated ΔT_m values (25.7 °C and 22.3 °C, respectively) are also higher than those obtained for other T4 lysozyme mutants. Typical values for single amino acid substitutions are in the 2–5 kcal/mol range for $\Delta\Delta G$ and 5–15 °C for ΔT_m. Although these values seems extraordinarily large, it should be noted that they correspond very nicely with the tight ts phenotype and the behavior of these mutant T4 lysozymes on petri plates. As noted earlier, no activity, in terms of plaque-forming ability, is seen at 43 °C. The T_m of WT T4 lysozyme at neutral pH is about 65°, so ΔT_m's in the range from −20 °C to −30 °C are as expected.

Another evidence of extreme reduced stability is the behavior of the mutant proteins during purification. The yields of the two mutant proteins were 10–20% of WT (which in our hands is normally 50–75 mg per 2.5-L culture). Unless proteolysis inhibitors are added immediately after cell lysis, a band of about 2 kDa lower in molecular weight appears on the SDS-polyacrylamide gel used to assess homogeneity. Also, for L66P, most of the protein seems to be in the form of an insoluble aggregate. We have attempted to recover active protein using techniques for purifying expressed protein from inclusion bodies, but have not been successful. We have obtained sufficient yields to perform enzyme activity assays and denaturation studies and to attempt protein crystallization for crystallographic analysis. When L91P was dialyzed against the low-salt buffer used for the urea denaturation experiments, the maximum concentration that could be obtained was 4.8 mg/mL, compared to more than 10 mg/mL for WT. Sauer et al. (1992) reported similar problems with the T4 lysozyme mutant V71P.

We have not been able to crystallize either mutant protein under standard WT conditions or any of the other crystallization conditions that have been used for T4 lysozyme mutants. We have also screened a wide range of other solvents and precipitants with no success thus far. The CD spectra (Fig. 2) show that no major conformational changes have occurred in the mutant proteins. Thus, we have used computer modeling to calculate the structure of the mutant proteins in order to try to determine the structural basis for the reduced stability of these mutants.

Table 2. *Comparisons of backbone atomic positions of the T4 lysozyme variants: X-ray crystal structures of WT (3LZM; Weaver & Matthews, 1987) and D72P (1L76; Sauer et al., 1992); simulated structures of WT, L66P, L91P, and D72P*[a]

	3LZM	1L76	WT	L91P	L66P	D72P
Comparison using residues 1–65, 67–90, and 92–164 (1,296 atoms)						
3LZM	–	0.37	1.45	1.74	1.22	–
1L76	0.37	–	–	–	–	1.12
WT	1.23	–	**0.84**	1.45	1.54	1.45
L91P	1.06	–	1.17	**1.21**	1.76	–
L66P	1.06	–	1.10	0.93	**0.85**	–
D72P	–	1.06	1.14	–	–	**0.80**
Comparison using residues 1–65 (520 atoms)						
3LZM	–	0.19	1.15	1.29	1.16	–
1L76	0.19	–	–	–	–	1.04
WT	1.05	–	**0.68**	1.32	1.50	1.09
L91P	0.86	–	0.97	**0.75**	1.63	–
L66P	0.91	–	1.08	0.83	**0.71**	–
D72P	–	0.93	0.88	–	–	**0.55**
Comparison using residues 67–90 and 92–164 (776 atoms)						
3LZM	–	0.32	1.24	1.46	1.17	–
1L76	0.32	–	–	–	–	0.84
WT	0.99	–	**0.64**	1.18	1.28	1.15
L91P	0.87	–	0.70	**1.08**	1.48	–
L66P	1.01	–	0.77	0.87	**0.69**	–
D72P	–	0.80	0.70	–	–	**0.45**

[a] Values in Å. Backbone atoms as listed were superimposed using the Superimpose command of Insight II (1993). RMSD between the two coordinate sets is calculated after a least-squares determination of the optimum superposition. For the simulated structures, the elements in boldface type on the diagonal are the comparisons between the 10–20-ps average structure and the 20–40-ps average structure. Below the diagonal, the 10–20-ps average structure is used. Above the diagonal, the 20–40-ps average structure is used.

L91P

Refer to Figure 4 and Kinemage 1 (from the 10–20-ps average structure). In the WT structure, the amide group of residue 91 makes a long hydrogen bond (N···O distance: 3.6 Å) with the carbonyl group of residue 87 to terminate the 84–90 α-helix. The carbonyl group of residue 87 also makes a hydrogen bond with the hydroxyl group of Ser 90 (O···O distance: 3.2 Å), exhibiting the n to $n-4$ hydrogen bonding back of serines and threonines (Baker & Hubbard, 1984; Gray & Matthews, 1984). Clearly, in the mutant structure with a proline at position 91, where the nitrogen is part of the pyrillidone ring, the hydrogen bond involving the amide group cannot be made (N···O distance: 4.5 Å). In addition, because of simple steric considerations, the introduction of the pyrillidone ring forces the polypeptide chain to become more extended. This can be seen by the fact that, in the WT structure, the 91 CA to 87 O distance is 4.5 Å, whereas in the L91P simulated structure, the same distance is 5.4 Å. The consequence is that, in the mutant structure,

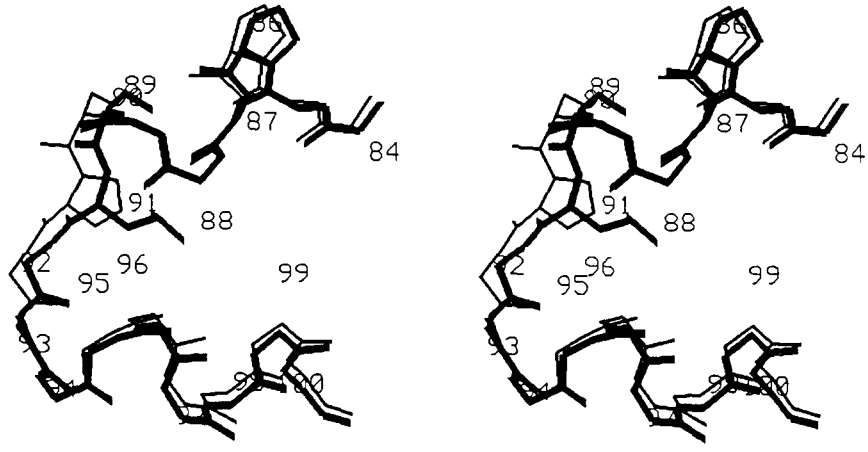

Fig. 4. Stereo view of the comparison of the simulated WT structure (thick lines) with the simulated L91P structure (thin lines) in the vicinity of residue 91. Shown are non-hydrogen backbone atoms for residues 84–100 and the side chains for residues 90 and 91. The figure was generated by InsightII (1993) from Biosym Technologies.

even the hydroxyl group of Ser 90 does not make a hydrogen bond with the carbonyl group of residue 87 (O···O distance: 4.2 Å). The bottom line is that, in the mutant structure, there is no hydrogen bonding partner for the backbone carbonyl oxygen of residue 87. According to an accessible surface area calculation using the program ACCESS (Richmond, 1984), the carbonyl oxygen of residue 87 is completely inaccessible in the WT crystal structure, the simulated WT structure, and the simulated L66P structure. It has an accessible surface area of 0.2 $Å^2$ (0.9%) in L91P. This "accessible" surface is the surface of the buried cavity and not on the external surface of the protein, and thus is not able to make a hydrogen bond with surface solvent molecules. Such unsatisfied hydrogen bonds have been found to be worth between 1 and 3 kcal/mol (Alber et al., 1987; Shirley et al., 1992; Chen et al., 1993). In addition, the carbonyl of residue 87 makes an unfavorable close contact with the pyrillidone ring of proline 91 (O···CD distance: 3.1 Å). This bad contact is believed to be a significant contributor to the destabilizing effect of proline in an α-helix (Yun et al., 1991). The folded form of a protein is stabilized by 0.5–1.0 kcal/mol when a proline is introduced into a structurally nondisruptive position due to the reduction of conformational entropy in the unfolded state (Matthews et al., 1987; Nicholson et al., 1992). Presumably, these three factors (loss of hydrogen bonding, introduction of the bad contact, and the conformational entropy) are taken into consideration in the various experiments that give a value of

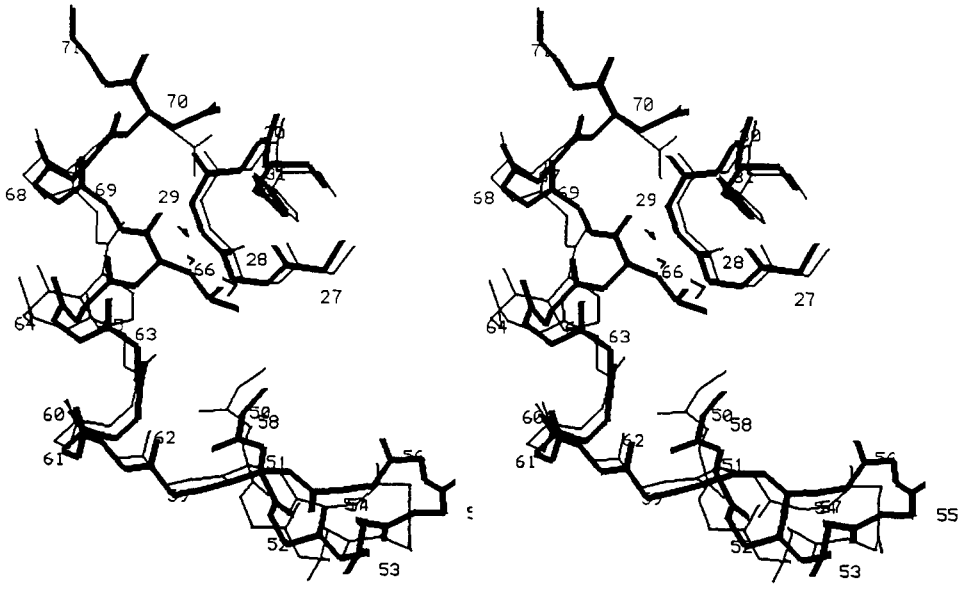

Fig. 5. Stereo view of the comparison of the simulated WT structure (thick lines) with the simulated L66P structure (thin lines) in the vicinity of residue 66. Shown are non-hydrogen backbone atoms for residues 26–30 and 50–71, the side chains for residues 66, 31, and 70 (the partially buried salt bridge), and the three water molecules occupying the pocket. The figure was generated by InsightII (1993) from Biosym Technologies.

3.4 kcal/mol for the the cost of introducing a proline into an α-helix (O'Neil & DeGrado, 1990; Yun et al., 1991; Sauer et al., 1992).

Leucine has a higher octanol to water free energy of transfer than does proline (Leu: 2.32 kcal/mol; Pro: 0.98 kcal/mol) (Fauchere & Pliska, 1983). On this consideration, because the side chain of residue 91 is buried, there is a 1.3 kcal/mol destabilization of the L91P mutant compared to the T4L WT.

The most striking feature of the mutant structure is the large cavity in the position occupied by the leucine side chain in the WT structure (Fig. 6). In the WT structure, the leucine side chain protrudes into the hydrophobic core and makes contact with the side chains of residues 87, 88, 95, 96, 121, 122, 126, and 153. After 20 ps and still after 40 ps of the simulation, there is no significant rearrangement of the hydrophobic core residues to fill this cavity, nor is there movement of water molecules from the molecular surface into the cavity. The volume of this cavity as determined by the program VOIDOO (Kleywegt & Jones, 1994) is 63.2 $Å^3$. Reduction of protein stability has been correlated with the introduction of a cavity into the hydrophobic core of a protein. Eriksson et al. (1992) reported that each cubic Ångstrom of cavity volume contributed to a 24-33 cal mol^{-1} $Å^{-3}$ reduction in stability. By this measure, the 63.2 $Å^3$ cavity introduced as a result of the leucine to proline substitution contributes to a reduction in stability of 1.5-2.1 kcal/mol.

The experimental value for the difference in stability between the WT and the L91P mutant is 8.2 kcal/mol. The features observed in the simulated mutant structure, together with correlations between structural features and stability in other systems, account for the 6.2-6.8 kcal/mol of the reduction of stability.

L66P

Refer to Figure 5 and Kinemage 2 (from the 10-20-ps average structure). In the WT structure, the amide group of residue 66 makes a hydrogen bond (N···O distance: 3.4 Å) with the carbonyl group of residue 62 and is in the middle of the long interdomain α-helix composed of residues 60-80. In the mutant structure with a proline at position 66, where the nitrogen is part of the pyrillidone ring, this hydrogen bond cannot be made (N···O distance: 5.3 Å). In the simulated mutant structure, it appears that the helix is becoming somewhat unraveled. Helical hydrogen bonds are not made for residues 62-65. This can be seen by comparing the distance between the amide N and the carbonyl oxygen, which form the helical hydrogen bond in the WT structure. For 62-66, the N···O distance is 3.4 Å for WT, but 4.9 Å for L66P. This is the hydrogen bond most obviously affected by the presence of the proline residue. However, the disruption of the helical hydrogen bonds continues for three additional residues: for 63-67, the N···O distance is 3.6 Å for WT, but 4.4 Å for L66P; for 64-68, it is 3.1 Å for WT, but 3.8 Å for L66P; for 65-69, it is 3.5 Å for WT, but 4.1 Å for L66P. The helix disruption is also evident from the phi-psi angles for residues 62-64, which in the mutant structure deviate significantly from α-helical values. The helix is disrupted such that residues 59-65 form one segment of helix and residues 66-80 form a second segment.

It is difficult to assess the effect of this helix disruption. Presumably, the same 3.4 kcal/mol for the the cost of introducing a proline into an α-helix that was discussed above will be present here, especially if no new hydrogen bonding partner is introduced for the carbonyl carbon of residue 62. According to ac-

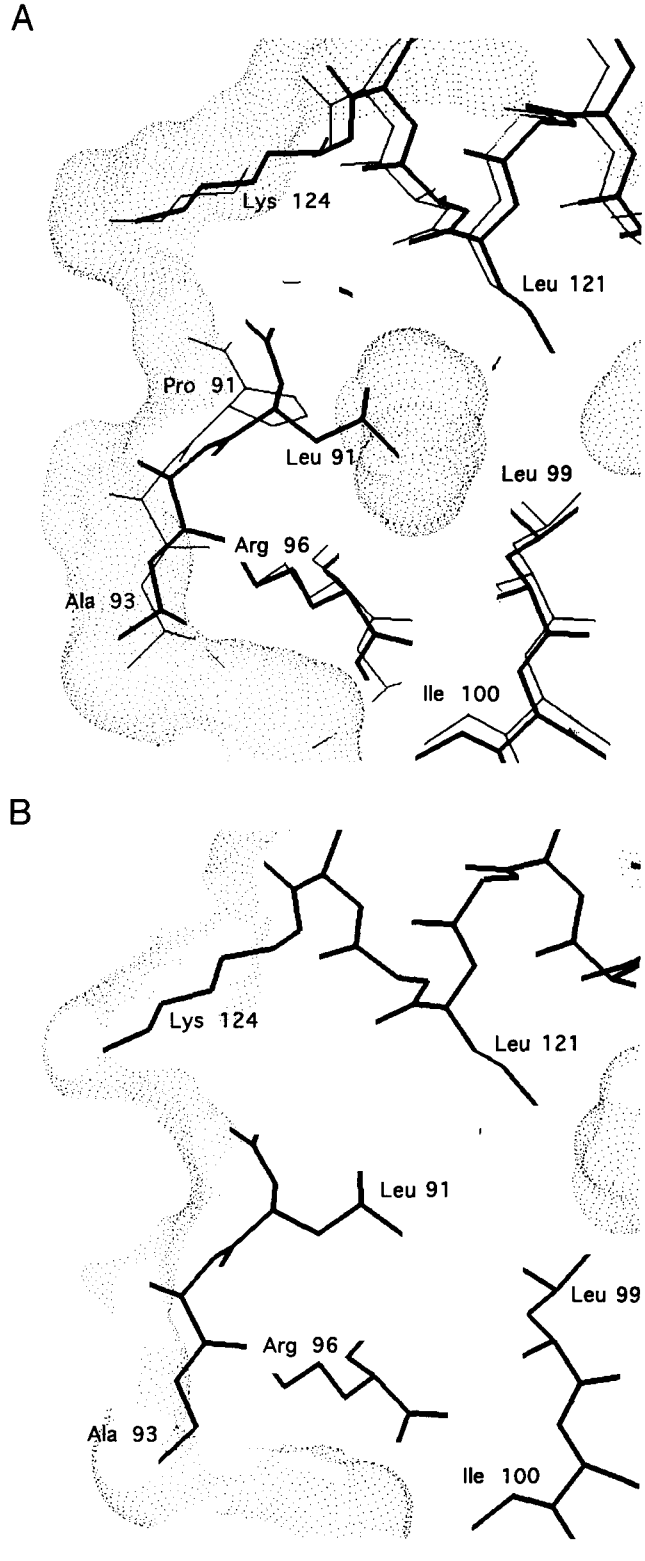

Fig. 6. A: Slab (5 Å) of the accessible surface of the simulated L91P structure (thin lines) showing the buried cavity found in the vicinity of residue 91. Surface is displayed at a density of 20 dots/$Å^2$. Simulated WT structure (thick lines) is shown superimposed onto the L91P structure. Cavity in the L91P mutant structure is located in the same position as the terminal methyl groups of the WT structure. The figure was generated by InsightII (1993) from Biosym Technologies. **B.** As in Figure 6A, but the accessible surface is from the simulated WT structure (thick lines) showing that no cavity exists in the WT structure.

cessible surface area calculation using the program ACCESS (Richmond, 1984), the carbonyl oxygen of residue 62 is completely inaccessible in the WT crystal structure and the simulated WT structure. It has an accessible surface area of 3.2 Å^2 (20.0%) in the simulated L66P structure, however, the nearest water molecule in the average simulated structure is 4.5 Å. Thus, this carbonyl oxygen has no hydrogen bonding partner in the folded structure. Other helical hydrogen bonds have been broken in addition to the one directly involved in the proline substitution. The carbonyl oxygen from residue 64 makes a hydrogen bond with a surface water molecule and the carbonyl oxygen from residue 65 makes a hydrogen bond with the amide nitrogen from residue 68 in a 3_{10}-like helical interaction. The carbonyl oxygen from residue 63 does not seem to have any hydrogen bonding partners in the folded structure. This carbonyl oxygen is completely solvent inaccessible in the WT crystal structure and has an accessible surface area of 0.2 Å^2 in the simulated WT structure. It has an accessible surface area of 1.6 Å^2 (6.3%) in the simulated L66P structure; the nearest water molecule is 4.8 Å too far for a hydrogen bond. As noted earlier, such unsatisfied hydrogen bonds have been found to be worth between 1 and 3 kcal/mol (Alber et al., 1987; Shirley et al., 1992; Chen et al., 1993).

The side chain of leucine 66 is nearly completely buried in the WT structure. In the L66P structure, there is a surface pocket that penetrates deeply into the hydrophobic region of the N-terminal domain (see Fig. 7). This is largely as a result of the space in the WT structure that is occupied by the terminal methyl groups of leucine, which is not being occupied with proline in that position. Additional space is created by the unraveling of the helix in the vicinity of residue 66. During the course of the simulation, this deep pocket is filled by three water molecules (1608, 1783, 1892) and these remain for the duration of the simulation. Deepest into the pocket is water 1608, which is hydrogen bonded to the amide nitrogen of residue 29 and to the other two pocket water molecules. A fourth possible hydrogen bond could be made with the carbonyl oxygen of residue 62 or 63, although the O···O distance is too long (4.5 Å and 4.8 Å, respectively) for a normal hydrogen bond. These carbonyl oxygens are part of the disrupted region of α-helix and do not make normal intrahelical hydrogen bonds. Water 1783 is hydrogen bonded to the other two pocket waters, the carbonyl oxygen of residue 66 and the carboxylate group of Asp 70. Water 1892 is hydrogen bonded to the other two pocket waters and makes long hydrogen bonds with the carbonyl oxygen of residue 62 (4.5 Å) and the nitrogen of the imidazole ring of His 31 (4.8 Å).

Again, it is difficult to assess the effect this pocket hydrogen bonding network on the stability of T4L. However, it is noteworthy that this new pocket penetrates into the core of T4L in the immediate vicinity of the partially buried salt bridge between Asp 70 and His 31. This salt bridge is believed to contribute 3.0–5.0 kcal/mol to the stability of T4L (Anderson et al., 1990). Additional water molecules near this salt bridge may increase the local dielectric constant and reduce its stabilizing effect. The 20–40-ps average structure shows essentially the identical features as the 10–20-ps structure. Interestingly, water 1783 and 1892 appear to have switched positions at some point during the simulation, but their interactions are such that the hydrogen bonding network described for the 10–20-ps structure is preserved.

The experimental value for the difference in stability between the WT and the L66P mutant is 7.1 kcal/mol. The features ob-

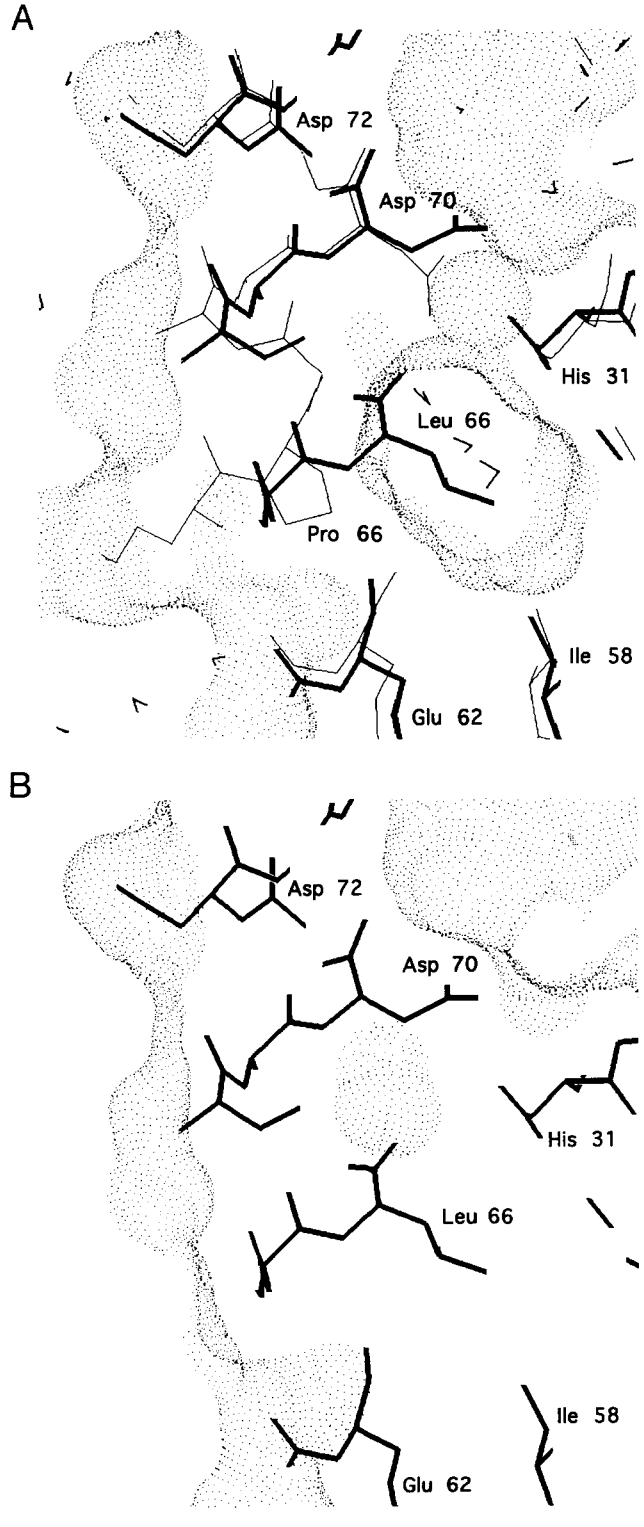

Fig. 7. A: Slab (5 Å) of the accessible surface of the simulated L66P structure (thin lines) showing the deep water occupied pocket found in the vicinity of residue 66. Surface is displayed at a density of 20 dots/Å^2. Simulated WT structure (thick lines) is shown superimposed onto the L66P structure. Pocket in the L66P mutant structure is located near the same position as the terminal methyl groups of the WT structure. The figure was generated by InsightII (1993) from Biosym Technologies. **B:** As in Figure 7A, but the accessible surface is from the simulated WT structure (thick lines) showing the absence of the pocket in the WT structure.

served in the simulated mutant structure, together with correlations between structural features and stability in other systems, account for the 4.9–5.5 kcal/mol of the reduction of stability, together with whatever reduction there might be in the stabilizing effect of the Asp 70 to His 31 salt bridge.

Materials and methods

Mutagenesis and selection

Mutagenesis was performed as described in Grütter et al. (1987) with 2-aminopurine as the mutagen. To select for "tight" ts mutants, *Escherichia coli* B-1 were grown to 1×10^8/mL, concentrated by centrifugation, resuspended in supplemented M9 medium (Okada et al., 1972) (supplement is Casamino acids (0.5%) and tryptophan (0.02 mg/mL)) to 4×10^8/mL at 43 °C, and infected with mutagenized phage at a multiplicity of infection of 10^{-3}. The temperature during phage growth was kept at 43°. After 3 min, 0.1 mL of phage T4 antisera ($K = 4{,}400$; from the late G. Streisinger) was added to inactivate unadsorbed T4 particles and and progeny phage released after a round of growth. Three minutes later, the tube was diluted 4× with supplemented M9 medium. Twenty minutes after infection, chloroform was added and the suspension was kept at 43° for 10 more minutes. The cells were placed on ice for 10 min, then washed two times. Hen eggwhite lysozyme was added to 200 μg/mL, and the phage plated immediately at 0.5 mL, 0.05 mL, and 0.05 mL of a 10× dilution per plate. The resultant plaques were picked and stabbed onto three plates: one incubated at 33°, one at 43°, and one incubated at 43° supplemented with hen eggwhite lysozyme on citrate agar (agar supplemented to 0.05 M Tris-HCl and 0.25% sodium citrate dihydrate). Phage strains growing at 33°, not at 43°, but at 43° in the presence of hen eggwhite lysozyme, were saved as tight ts mutants.

Identification of the mutations

Preparation of DNA suitable for cloning was carried out as described in Grütter et al. (1987), summarized as follows. The tight ts mutation was crossed into T4 *56^{am}denA$^-$denB$^-$* to produce unmodified cytosine-containing DNA suitable for cloning (Owen et al., 1983) A ~4-kb *Xho* I restriction fragment containing the T4 lysozyme gene was purified using agarose gel electrophoresis. The *Xho* I fragment was removed from the agarose by electroelution or by the quick-freeze method (Bensen, 1984). For the mutant strain *T1* (later identified as L91P), the 4-kb fragment was digested with *Eco*R I and *Hin*d III and cloned into similarly restricted M13mp8. For all other mutant strains, the 4-kb fragment was digested with *Xba* I and *Hin*d III and cloned into similarly restricted M13mp18. The DNA sequence of the noncoding strand was determined by the chain termination method (Sanger et al., 1977) using the 17-base M13 forward sequencing primer.

Expression of mutant protein and protein purification

DNA prepared from the M13 clones was subcloned into the T4 lysozyme expression plamid pHSe5 (Muchmore et al., 1989). The DNA coding for the L91P mutation was cloned into the expression plasmid by cloning the *Eco*R I–*Hin*d III fragment containing the 3′ end of the mutant lysozyme gene into the equivalent *Eco*R I–*Hin*d III region of the expression plasmid. The DNA coding for the L66P mutation was cloned as follows. M13 RF DNA containing the mutant gene coding for the L66P was digested with *Sna*B I, and the 333-bp *Sna*B I–*Sna*B I fragment coding for the central region of the T4 lysozyme gene was isolated by PAGE and separated from the gel by the method described in Sambrook et al. (1989). The *Sna*B I–*Sna*B I fragment was cloned into a pHSe5 that had been digested with *Sna*B I and religated to produce a version of the expression plasmid with the central portion (corresponding to residues 8–118 of the protein) of the T4 lysozyme gene deleted. Successful cloning and correct orientation was determined by testing liquid cultures for inducible lysozyme activity. WT and tight ts mutants of T4 lysozyme were purified to apparent homogeneity using a slightly modified version of the procedure of Muchmore et al. (1989). WT T4 lysozyme usually causes cell lysis, so, after centrifugation of the culture, the protein is found in the supernatant. L91P and L66P T4 lysozyme usually does not cause lysis. After centrifugation, the cells were resuspended in 0.1 M $NaPO_4$ buffer, pH 7.0, 0.2 M NaCl, 0.01 M $MgCl_2$, and 0.001 M $CaCl_2$. Lysis was induced by addition of EDTA to 0.005 M. The protease inhibitor PMSF was added to 0.1 μg/mL before centrifugation if lysis had occurred or following cell lysis. Clarified supernatant or lysed resuspended pellets were diluted by adding five volumes of distilled water containing 0.001 M 2-mercaptoethanol. The protein was purified using a CM-Sepharose column and further concentrated using an SP-Sephadex column.

Enzyme assays

Enzyme activities were determined by the turbidometric assay of Tsugita et al. (1968). Fifty milligrams of lyophilized *E. coli* B cells (Sigma) were suspended in 10 mL of 0.05 M Tris-HCl buffer, pH 7.4, followed by the addition of 1 mL of chloroform with vigorous mixing. The treatment with chloroform was found to be essential to obtain a competent lysozyme substrate. The bacterial cell suspension was diluted with the Tris buffer to give a solution with a final A_{450} of 0.7–0.8. Ten microliters of enzyme was added to 3 mL of the cell suspension and the decrease in absorbance monitored as a function of time by means of a chart recorder attached to a Varian dual beam UV/Vis spectrophotometer. Absorbance decreased linearly with time between values of 0.75 and 0.40. Significant deviations from linearity occurred when very low enzyme concentrations were used. In those cases, reported activities are the initial rates. Enzyme concentrations are of the 10-μL aliquot added, not taking into account the dilution into the 3-mL cell suspension. All assays were performed at 25 °C.

Thermal inactivation

Protein stability was determined by incubating the enzyme at 65 °C, removing 20-μL aliquots at various time intervals, and measuring the remaining activity by the turbidometric assay. Samples were immediately placed on ice and assayed within a few minutes. Under these conditions, denaturation appeared to be irreversible.

Urea-induced denaturation monitored by UV difference spectroscopy

Protein stability was also measured using urea-induced denaturation monitored by UV difference spectroscopy as described by

Matthews (1987b) and Pace (1986). The difference spectra between T4 lysozyme exposed to various urea concentrations and T4 lysozyme in the absence of urea were obtained using tandem double-compartment rectangular cells (10-mm-pathlength). The background spectra were taken from a tandem cell containing protein (1 mg/mL) and buffer (0.010 M KPO4 buffer, pH 7.0, 0.004 M EDTA, 0.001 M 2-mercaptoethanol) in one of the compartments and urea and buffer in the other. The experimental spectra were taken from a tandem cell containing protein, urea, and buffer (same concentrations as in the background cell) in one of the compartments and only buffer in the other. The resulting difference spectra are measurements of the change in absorbance due to denaturation of the protein by urea. Absorbances at 291.3 nm were recorded using a Perkin Elmer Lambda Array 3840 UV/VIS spectrophotometer. Data were processed assuming a two-state model. Using the data analysis program Igor (1988), the data was fit to the following six-parameter function:

$$A_{291.3} = F - (F - U) * \frac{e^{(m*[\text{urea}] - \Delta G)/RT}}{1 + e^{(m*[\text{urea}] - \Delta G)/RT}} \quad (1)$$

where $F = FM*[\text{urea}] + FB$ and $U = UM*[\text{urea}] + \text{UB}$ are the linear solvent perturbation effect expressions for the folded and unfolded conformation, respectively (*FM* and *UM* being the slope of that line and *FB* and *UB* being the intercept); *m* is the slope of the linear extrapolation to 0 M urea of the ΔG dependence upon urea concentration; ΔG is the free energy in kcal/mol of the unfolding reaction. The slopes of the baselines were constrained manually to be positive.

CD spectroscopy

Spectra were measured on an Aviv 62DS spectropolarimeter. The protein was in 0.010 M potassium phosphate buffer, pH 6.78, 0.15 M KCl, 0.001 M 2-mercaptoethanol. Protein concentrations were 0.2675 mg/mL for WT, 0.0757 mg/mL for L66P, and 0.0461 mg/mL for L91P, as determined by the Bradford protein assay (Bradford, 1976) or by UV absorption at 280 nm (ϵ_{280} = 22,784 M^{-1} cm^{-1}). A 0.1-cm pathlength was used for WT and a 0.5-cm pathlength was used for L66P and L91P. The residue ellipticity (θ) was calculated using a molecular weight of 17,800 Da and 164 amino acid residues.

Computer modeling

Energy minimization and molecular dynamics simulations were performed with Discover (1993) using the CFF91 forcefield running on a Silicon Graphics Indigo^2 computer graphics workstation. The WT X-ray coordinates (3LZM) were used as the starting coordinates (Weaver & Matthews, 1987). Hydrogens were added assuming the typical ionization state of each group at pH 7.0. His 31 was given a +1 charge (Anderson et al., 1990). A pseudo-unit cell of dimensions 46.0 Å × 46.0 Å × 56.0 Å was created with a single protein molecule at the center and filled with 2,787 water molecules. The structure was inspected to find charged groups that were not paired with an oppositely charged group. In order to achieve charge neutrality for the unit cell, water molecules near the unpaired groups were changed to a sodium ion or to a chloride ion. The minimum image periodic boundary conditions (MIPBC) were used for all calculations. The cutoff distance for nonbonded interactions was set at 16 Å with a 0.0-Å switch distance (Kitson et al., 1993). Initially, crystallographically determined positions were held fixed to allow for energy minimization with respect to the hydrogen positions and to the solvent. After that initial stage, the position of backbone atoms were fixed and side-chain atoms, hydrogens, and the solvent atoms were allowed to move. Finally, all atoms were allowed to move freely. Starting with the energy-minimized WT structure, the mutant proteins L91P, L66P, and D72P were built and further cycles of energy minimization carried out to relieve any unfavorable interactions introduced in making the substitution. The 40-ps molecular dynamics simulations were conducted on each of the four structures. Coordinates were saved at 200-fs intervals during the course of the simulation. The saved structures for the 10–20-ps and 20–40-ps segments of each simulation were averaged to give the 10–20-ps and 20–40-ps average structures for analysis.

Acknowledgments

This work was supported in part by several grants to T.M.G.: a Bristol-Myers Company Grant of Research Corporation, an Academic Research Enhancement Award from the National Institutes of Health (1R15 GM42074-01), a Calvin Research Fellowship, and a Calvin College-Howard Hughes Medical Institute Faculty Research Opportunities Award. We thank Brian Matthews and his group at the University of Oregon for bacterial and viral strains used in this work. This project was begun while T.M.G. was a graduate student in the Matthews laboratory. CD spectra were done at the Department of Medical Biochemistry and Genetics at Texas A&M University with the kind assistance of Dr. J. Martin Scholtz.

References

Alber T, Bell JA, Dao-Pin S, Nicholson H, Wozniak JA, Cook S, Matthews BW. 1988. Replacements of Pro86 in phage T4 lysozyme extend an α-helix but do not alter protein stability. *Science 239*(4840):631–635.

Alber T, Sun DP, Wilson K, Wozniak JA, Cook SP, Matthews BW. 1987. Contributions of hydrogen bonds of Thr 157 to the thermodynamic stability of phage T4 lysozyme. *Nature 330*(6143):41–46.

Anderson DE, Becktel WJ, Dahlquist FW. 1990. pH-Induced denaturation of proteins: A single salt bridge contributes 3–5 kcal/mol to the free energy of folding of T4 lysozyme. *Biochemistry 29*:2403–2408.

Arnold GE, Manchester JI, Townsend BD, Ornstein RL. 1994. Investigation of domain motions in bacteriophage T4 lysozyme. *J Biomol Struct Dyn 12*:457–474.

Baker EN, Hubbard RE. 1984. Hydrogen bonding in globular proteins. *Prog Biophys Mol Biol 44*:97–179.

Barlow DJ, Thornton JM. 1988. Helix geometry in proteins. *J Mol Biol 201*:601–619.

Becktel WJ, Schellman JA. 1987. Protein stability curves. *Biopolymers 26*: 1859–1877.

Bensen SA. 1984. A rapid procedure for isolation of DNA fragments from agarose gels. *BioTechniques 2*:66–67.

Blaber M, Zhang XJ, Lindstrom JD, Pepiot SD, Baase WA, Matthews BW. 1994. Determination of α-helix propensity within the context of a folded protein. Sites 44 and 131 in bacteriophage T4 lysozyme. *J Mol Biol 235*:600–624.

Bradford M. 1976. A rapid and sensitive method for the quantitation of microgram quantities of protein utilizing the principle of protein-dye binding. *Anal Biochem 72*:248.

Chen YW, Fersht AR, Henrick K. 1993. Contribution of buried hydrogen bonds to protein stability. The crystal structures of two barnase mutants. *J Mol Biol 234*:1158–1170.

Discover. 2.9/3.1. 1993. San Diego, California: Biosym Technologies, Inc.

Dixon MM, Nicholson H, Shewchuk L, Baase WA, Matthews BW. 1992. Structure of a hinge-bending bacteriophage T4 lysozyme mutant, Ile3.fwdarw.Pro. *J Mol Biol 227*:917–933.

Eriksson AE, Baase WA, Zhang XJ, Heinz DW, Blaber M, Baldwin EP, Mat-

thews BW. 1992. Response of a protein structure to cavity-creating mutations and its relation to the hydrophobic effect. *Science 255*(5041): 178–183.

Faber HR, Matthews BW. 1990. A mutant T4 lysozyme displays five different crystal conformations. *Nature 348*(6298):263–266.

Fauchere JL, Pliska V. 1983. Hydrophobic parameters *p* of amino acid side chains from the partitioning of *N*-acetyl-amino acid amides. *Eur J Med Chem Chim Ther 18*:369–375.

Gray TM, Matthews BW. 1984. Intrahelical hydrogen bonding of serine, threonine and cysteine residues within α-helixes and its relevance to membrane-bound proteins. *J Mol Biol 175*:75–81.

Grütter MG, Gray TM, Weaver LH, Alber T, Wilson K, Matthews BW. 1987. Structural studies of mutants of the lysozyme of bacteriophage T4. The temperature-sensitive mutant protein Thr 157 → Ile. *J Mol Biol 197*: 315–329.

Heinz DW, Baase WA, Zhang XJ, Blaber M, Dahlquist FW, Matthews BW. 1994. Accommodation of amino acid insertions in an α-helix of T4 lysozyme. Structural and thermodynamic analysis. *J Mol Biol 236*:869–886.

Igor. 1.26. 1988. Lake Oswego, Oregon: WaveMetrics.

Insight II. 2.20. 1993. San Diego, California: Biosym Technologies, Inc.

Kitson DH, Avbelj F, Moult J, Nguyen DT, Mertz JE, Hadzi D, Hagler AT. 1993. On achieving better than 1-Å accuracy in a simulation of a large protein: *Streptomyces griseus* protease A. *Proc Natl Acad Sci USA 90*:8920–8924.

Klemm JD, Wozniak JA, Alber T, Goldenberg DP. 1991. Correlation between mutational destabilization of phage T4 lysozyme and increased unfolding rates. *Biochemistry 30*:589–594.

Kleywegt GJ, Jones TA. 1994. Detection, delineation, measurement and display of cavities in macromolecular structures. *Acta Crystallogr D 50*:178–185.

Matthews BW. 1987a. Genetic and structural analysis of the protein stability problem. *Biochemistry 26*:6885–6888.

Matthews BW, Nicholson H, Becktel WJ. 1987. Enhanced protein thermostability from site-directed mutations that decrease the entropy of unfolding. *Proc Natl Acad Sci USA 84*:6663–6667.

Matthews CR. 1987b. Effect of point mutations on the folding of globular proteins. *Methods Enzymol 154*:498–511.

Muchmore DC, McIntosh LP, Russell CB, Anderson DE, Dahlquist FW. 1989. Expression and nitrogen-15 labeling of proteins for proton and nitrogen-15 nuclear magnetic resonance. *Methods Enzymol 177*: 44–73.

Nicholson H, Tronrud DE, Becktel WJ, Matthews BW. 1992. Analysis of the effectiveness of proline substitutions and glycine replacements in increasing the stability of phage T4 lysozyme. *Biopolymers 32*:1431–1441.

Okada Y, Streisinger G, Owen J, Newton J, Tsugita A, Inouye M. 1972. Molecular basis of mutational hot spot in the lysozyme gene of bacteriophage T4. *Nature 236*(5346):338–341.

O'Neil KT, DeGrado WF. 1990. A thermodynamic scale for the helix-forming tendencies of the commonly occurring amino acids. *Science 250*:646–651.

Owen JE, Schultz DW, Taylor A, Smith GR. 1983. Nucleotide sequence of the lysozyme gene of bacteriophage T4. Analysis of mutations involving repeated sequences. *J Mol Biol 165*:229–248.

Pace CN. 1986. Determination and analysis of urea and guanidine hydrochloride denaturation curves. *Methods Enzymol 131*:266–280.

Richmond TJ. 1984. Solvent accessible surface area and excluded volume in proteins. Analytical equations for overlapping spheres and implications for the hydrophobic effect. *J Mol Biol 178*:63–89.

Sambrook J, Fritsch EF, Maniatis T. 1989. *Molecular cloning, 2nd ed.* Cold Spring Harbor, New York: Cold Spring Harbor Laboratory Press.

Sanger F, Nicklen S, Coulson AR. 1977. DNA sequencing with chain-terminating inhibitors. *Proc Natl Acad Sci USA 74*:5463–5467.

Sauer UH, Sun DP, Matthews BW. 1992. Tolerance of T4 lysozyme to proline substitutions within the long interdomain α-helix illustrates the adaptability of proteins to potentially destabilizing lesions. *J Biol Chem 267*: 2393–2399.

Shirley BA, Stanssens P, Hahn U, Pace CN. 1992. Contribution of hydrogen bonding to the conformational stability of ribonuclease T1. *Biochemistry 31*:725–732.

Streisinger G, Mukai F, Dreyer WJ, Miller B, Horiuchi S. 1961. Mutations affecting the lysozyme of phage T4. *Cold Spring Harbor Symp Quant Biol 26*:25–30.

Tsugita A, Inouye M, Terzaghi E, Streisinger G. 1968. Purification of bacteriophage T4 lysozyme. *J Biol Chem 243*:391–397.

Weaver LH, Matthews BW. 1987. Structure of bacteriophage T4 lysozyme refined at 1.7 Å resolution. *J Mol Biol 193*:189–199.

Yun RH, Anderson A, Hermans J. 1991. Proline in α-helix: Stability and conformation studied by dynamics simulation. *Proteins Struct Funct Genet 10*:219–228.